ACS Sustainable Chemistry & Engineering

Research Article

Cite This: ACS Sustainable Chem. Eng. 2018, 6, 2612−2620

Ternary Mixtures of Sulfolanes and Ionic Liquids for Use in High-Temperature Supercapacitors

Stephen Fletcher,[†] Iain Kirkpatrick,[*,‡] Rob Thring,[‡] Roderick Dring,[§] Joshua L. Tate,[§] Harry R.M. Geary,[§] and Victoria Jane Black[§]

[†]The Fletcher Consultancy, Loughborough, Leicestershire LE11 3LU, United Kingdom

[‡]Department of Aeronautical and Automotive Engineering and [§]Department of Chemistry, Loughborough University, Epinal Way, Loughborough, Leicestershire LE11 3TU, United Kingdom

ABSTRACT: Ionic liquids are a natural choice for supercapacitor electrolytes. However, their cost is currently high. In the present work, we report the use of ternary mixtures of sulfolane, 3-methyl sulfolane, and quaternary ammonium salts (quats) as low-cost alternatives. Sulfolane was chosen because it has a high Hildebrand solubility parameter (δ_H = 27.2 $MPa^{1/2}$) and an exceptionally high dipole moment (μ = 4.7 D), which means that it mixes readily with ionic liquids. It also has a high flash point (165 °C), a high boiling point (285 °C), and a wide two-electrode (full-cell) voltage stability window (>7 V). The only problem is its high freezing point (27 °C). However, by using a eutectic mixture of sulfolane with 3-methyl sulfolane, we could depress the freezing point to −17 °C. A second goal of the present work was to increase the electrical conductivity of the electrolyte beyond its present-day value of 2.1 mS cm^{-1} at 25 °C, currently provided by butyltrimethylammonium bis(trifluoromethylsulfonyl)imide (BTM-TFSI). We explored two methods of doing this: (1) mixing the ionic liquid with the sulfolane eutectic and (2) replacing the low-mobility TFSI anion with the high-mobility MTC anion (methanetricarbonitrile). At the optimum composition, the conductivity reached 12.2 mS cm^{-1} at 25 °C.

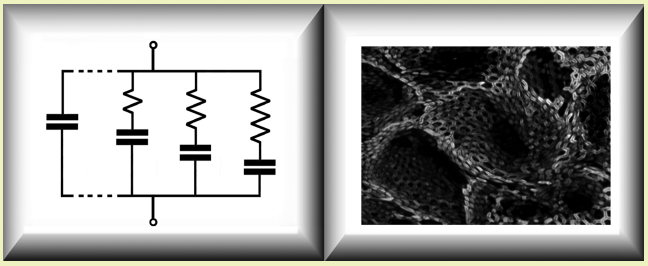

KEYWORDS: *Supercapacitor, Ionic liquid, Sulfolane, Eutectic, Conductivity, Activated carbon*

INTRODUCTION

One of the most promising strategies for decreasing noxious emissions caused by the global transportation network (motor vehicles, railroad engines and aircraft) is to replace today's petroleum-based fuels with electrochemical power sources, such as supercapacitors, fuel cells, and batteries. A compelling feature of electrochemical power sources is their ability to convert chemical energy into electrical energy without the need for combustion, thus opening the door to "low-carbon" operation. While it is indeed true that many electrochemical technologies are environmentally benign, they also suffer from certain limitations with regard to thermal stability, chemical stability, cycle life, and cost. Intense efforts are therefore underway around the world to improve them.

In the UK, the ELEVATE consortium was recently established by the Engineering and Physical Sciences Research Council (EPSRC) to speed up the development of low-carbon vehicle technologies.[1] A strategic goal of this consortium is to recognize, characterize, and optimize new materials for high-temperature supercapacitors. The present work summarizes our progress in that direction.

Thermal management of supercapacitors becomes an increasingly important issue as their size increases. Although they are not heat engines, supercapacitors nevertheless release heat due to the passage of electric current through their internal resistance, and so they must be constructed from heat-tolerant materials. Therein lies a problem. Present-day supercapacitors generally cannot operate above 65 °C due to the presence of volatile solvents such as acetonitrile (boiling point (bp) 82 °C). To withstand higher temperatures, less-volatile solvents such as ionic liquids must be used.[2] By definition, ionic liquids are solvent-free combinations of anions and cations that display at least one liquid-like phase below 350 °C.[3,4] Given the right cation/anion combination, ionic liquids can strongly resist thermal decomposition, although some care is needed in making the correct choice.

The world's first patent for a high-temperature supercapacitor was filed in June 2012 and granted in April 2016.[5] This disclosed an ionic liquid electrolyte (optionally gelled with fumed silica nanoparticles) and an operating range of at least 20−220 °C. Because the voltage stability windows of ionic liquids invariably decrease with increasing temperature, the patent focused on those ionic liquids that have exceptionally wide voltage stability windows at room temperature. In a preferred embodiment, the patent specified the combination of tetraalkylammonium (TAA) cations and bis(trifluoromethylsulfonyl)imide (TFSI) anions. Systematic measurements had revealed that increasing the chain lengths

Received: November 7, 2017
Revised: December 6, 2017
Published: December 14, 2017

DOI: 10.1021/acssuschemeng.7b04117
ACS Sustainable Chem. Eng. 2018, 6, 2612−2620

Table 1. Physical Properties of Some Industrial Aprotic Solvents[a]

		mp (°C)	bp (°C)	D	δ_H (MPa$^{1/2}$)	flash point (°C)	relative permittivity ε_r	vapor pressure (Pa)
Sulfolane	S	+27	285	4.7	27.2	165	43 (30 °C)	16 (50 °C)
3-methylsulfolane	3-MS	−2	279	4.8	25.4	154	29 (30 °C)	n/a
N-methyl-2-pyrrolidone	NMP	−24	202	3.92	22.9	86	32 (25 °C)	40 (25 °C)
dimethylsulfoxide	DMSO	+16	189	3.96	26.7	85	46 (25 °C)	60 (20 °C)
N,*N*-dimethylacetamide	DMAC	−20	165	3.81	22.7	63	37 (25 °C)	330 (20 °C)
N,*N*-dimethylformamide	DMF	−61	153	3.86	24.8	58	37 (25 °C)	350 (20 °C)

[a]D is the dipole moment. δ_H is the Hildebrand solubility parameter. Hildebrand values mainly from ref 6. The Hildebrand values for ionic liquids generally fall in the range 20−26 MPa$^{1/2}$. Other data are from refs 7−10. ***Caution**: All solvents listed are potential skin/eye irritants.*

of the alkyl groups increased the voltage stability windows at the cost of decreased electrical conductivity. A compromise was therefore reached by combining the butyltrimethylammonium (BTM) cation with the bis(trifluoromethylsulfonyl)imide (TFSI) anion. The resulting ionic liquid (BTM-TFSI) had a two-electrode (full-cell) voltage stability window of 7 V at 25 °C, falling to 3.5 V at 200 °C. At the same time, the electrical conductivity κ rose from 2.1 mS cm^{-1} at 25 °C to 57 mS cm^{-1} at 200 °C.

Thermal analysis of ionic liquids was also carried out. This revealed that salts of symmetric tetraalkylammonium cations with TFSI, such as tetramethyl-, tetraethyl-, tetrapropyl-, and tetrabutyl-, all had melting points (mp) >96 °C, i.e. they were solids at room temperature, whereas asymmetric tetraalkylammonium cations such as butyltrimethyl- and hexyltriethyl- had freezing points <20 °C, i.e., they were liquids at room temperature. For this reason, the asymmetric cations were preferred for room-temperature operation.[3]

Although BTM-TFSI has subsequently proved an excellent electrolyte for high-temperature supercapacitors, it has not yet been manufactured on the large industrial scale, so its commercial cost is currently high. In order to decrease costs, we wondered whether it might be possible to incorporate an inexpensive diluent having the following properties: (i) a very high bp, (ii) a wide voltage stability window, and (iii) a high relative permittivity (so that it would mix with BTM-TFSI in all proportions). Ideally, such a solvent would also be halide-free (to protect the ozone layer), be aprotic (to prevent hydrogen evolution at negative potentials), and have a flash point >150 °C (to ensure thermal safety).

The physical properties of some industrial solvents that approach the desired criteria are compiled in Table 1. It can be seen that the cyclic sulfone known as sulfolane (see Figure 1) has the highest flash point and the highest bp. We therefore selected it for further study.

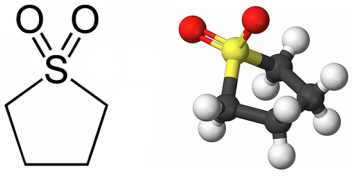

Figure 1. Structural formula of Sulfolane.

Patents for the industrial production of Sulfolane were first granted during the second World War.[11−13] These patents disclosed that sulfolane could be manufactured by the catalytic hydrogenation of sulfolene (2,5-dihydrothiophene-1,1-dioxide) which, in turn, could be manufactured from butadiene and sulfur dioxide. Shortly thereafter, the Shell Development Company disclosed that sulfolane could be employed as a highly selective solvent for the extraction of aromatic hydrocarbons (mainly benzene, toluene, and xylene) from petroleum refinery reformate.[14,15] Due to the high commercial value of the aromatics, more than 150 sulfolane extraction units have now been built.[16] Attractive properties of sulfolane as an industrial solvent are its high bp (285 °C) and its very slow rate of thermal decomposition, less than 0.05% per day at 200 °C.[17] Today, Sulfolane also finds widespread use in the Sulfinol process for scrubbing hydrogen sulfide (H_2S), carbonyl sulfide (COS), and organo-mercaptans (RSH) from natural gas.[18] The total worldwide production of sulfolane is estimated to be between 16 000 and 32 000 metric tonnes per year.[19]

Besides its resistance to thermal decomposition, sulfolane is also resistant to chemical and electrochemical oxidation. This is because the S-atom in sulfolane is already in the +6 oxidation state; therefore, it is reluctant to donate further electrons to an acceptor. As regards physicochemical properties, sulfolane has a high Hildebrand solubility parameter (δ_H = 27.2 MPa$^{1/2}$), a high relative permittivity (ε_r = 43), and an exceptionally high dipole moment (μ = 4.7 D). This unusual combination of properties makes it miscible with water, acetone, and toluene at 30 °C. Sulfolane is also capable of solvating cations via the oxygen atoms on the sulfone group, and is a good solvent for quaternary ammonium salts (quats), nitrocellulose, polyvinylchloride, and polystyrene.

There is, however, one important problem with pure sulfolane: It has a freezing point of 27 °C, so it tends to solidify at room temperature. To avoid this difficulty, we explored the possibility of lowering its freezing point by mixing it with one of its alkyl-substituted analogues, namely, 3-methylsulfolane. Values for the freezing point depression constant for several solutes in sulfolane are known to cluster around −65 K kg mol^{-1},[20] and 3-methylsulfolane is available commercially as a racemic mixture of two diastereoisomers, so hopes of obtaining a large freezing point depression were high. We were not disappointed.

A graph of freezing point versus mole fraction of (*R*,*S*)-3-methylsulfolane in sulfolane is shown in Figure 2. It can be seen that mixtures containing between 40 and 65 mol % of (*R*,*S*)-3-methylsulfolane had freezing points between −15 and −17 °C, a depression of more than 40 °C compared with that of the parent compound. Since (*R*,*S*)-3-methylsulfolane was slightly more expensive than sulfolane (though still much cheaper than an ionic liquid) we selected the 40 mol % eutectic mixture for further study. (The "eutectic" mixture is the one that freezes at the lowest temperature.)

An important commercial consideration in the design of supercapacitors is the long-term stability of the cations during charge/discharge cycling. In this regard, quaternary ammo-

DOI: 10.1021/acssuschemeng.7b04117
ACS Sustainable Chem. Eng. 2018, 6, 2612−2620

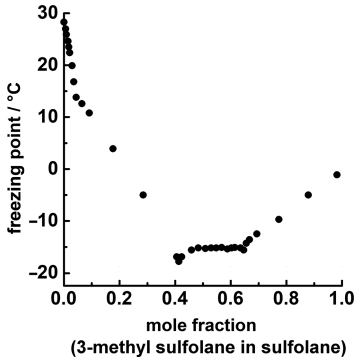

Figure 2. Freezing point versus mole fraction for mixtures of 3-methylsulfolane in sulfolane. Data from Chappelow et al.[21]

nium cations, sometimes known as quats, are of special interest. They have the generic formula NR_4^+, where R is an alkyl or aryl group, and their bulky size makes them nonelectrophilic. The four R groups are also able to shield the nitrogen atom against interfacial electron tunneling, which extends the voltage stability window.[3] However, it has long been known that quaternary ammonium cations can decompose in extreme circumstances. For example, if tetraalkyl ammonium cations are heated above 100 °C in a concentrated solution of hydroxide ions (and if they also contain N−C−C−H units), then they can undergo a classic β-elimination reaction (Hofmann Elimination) to yield an alkene, a tertiary amine, and water.[22−24] A Reverse Menshutkin reaction may also occur, yielding a tertiary amine.[25] Fortunately, both of these unwanted reactions can be prevented by pairing the quaternary ammonium cations with anions of strong Brønsted acids, because the latter are by definition poor nucleophiles. Two well-known examples are the fluorine-containing anion bis(trifluoromethylsulfonyl)-imide (TFSI) and the fluorine-free anion methanetricarbonitrile (MTC), which are shown in Figure 3. Both of these were studied in the present work.

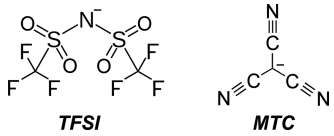

Figure 3. Two anions that display low nucleophilicity.[26,27] TFSI is bis(trifluoromethylsulfonyl)imide; MTC is methanetricarbonitrile. The latter is commonly referred to by its non-IUPAC name tricyanomethanide.

A much-desired goal of the present work was to raise the electrical conductivity κ of our supercapacitor electrolyte above its present-day value of 2.1 mS cm^{-1} at 25 °C, which is currently provided by butyltrimethylammonium bis-(trifluoromethylsulfonyl)imide (BTM-TFSI).[3−5] There were two main reasons for attempting this. First, an improved conductivity would decrease the ohmic (thermal) losses of real-world devices. Second, an improved conductivity would allow a deeper penetration of the capacitive charge/discharge reaction into the electrode pores, yielding a greater specific capacitance.[28]

Two possible methods of increasing the electrical conductivity of ionic liquids were considered: (1) The low-mobility TFSI anion could be replaced by a high-mobility anion.[29−31] (2) The ionic liquid could be mixed with a polar solvent.[32−37] Anticipating our main results, Figure 4 shows the

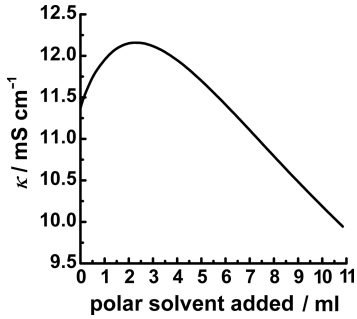

Figure 4. Conductivity κ of the ionic liquid BTM-MTC versus volume of polar solvent added. In this case the polar solvent was a 60/40 mol % eutectic mixture of sulfolane and 3-methylsulfolane (S/3MS). The initial volume of BTM-MTC was 10 mL, and the rate of continuous dilution was 5 mL h^{-1}. A conductivity maximum was observed at 67.5 mol % of ionic liquid. T = 25 °C. The 3960 points were recorded at 2 s intervals.

effect of replacing the TFSI anion with the MTC anion and then diluting the pure ionic liquid with the eutectic mixture of sulfolane and (*R*,*S*)-3-methylsulfolane (hereafter S/3MS). Changing the anion caused an immediate rise in conductivity from 2.1 to 11.4 mS cm^{-1}. Then, despite the fact that the ionic liquid was being diluted by polar solvent, the solution conductivity increased further to 12.2 mS cm^{-1}. In the latter case, a greater conductivity was being observed in a less concentrated solution! It is evident from these data that combinations of solvents and ionic liquids offer considerable scope for improved supercapacitor performance.

EXPERIMENTAL SECTION

Materials. Ionic liquids (>98% purity) were synthesized by Io-litec (Ionic Liquid Technologies GmbH, Salzstrasse 184, 74076 Heilbronn, Germany) and their purity was confirmed by ^{13}C NMR. All ionic liquids and solvents were dried at 130 °C for 24 h before use. Sulfolane (2,3,4,5-tetrahydrothiophene-1,1-dioxide, CAS [126−33−0], 99% purity) was purchased from Sigma-Aldrich Corporation (St. Louis, MO). (*R*,*S*)-3-Methylsulfolane (3-methyltetrahydrothiophene 1,1-dioxide, CAS [872−93−5], 98% purity) was purchased from Tokyo Chemical Industry (Tokyo, Japan).

Voltammetry. Voltammetry experiments were performed thermostatically in pyrex cells. Working electrodes were glassy carbon disks (d = 3.0 mm, Bioanalytical Systems, Inc.) shrink-fitted into glass-filled Teflon holders. Counter electrodes were manufactured in-house from platinum gauze (99.9%, 52-mesh, CAS 7440−06−4, Sigma-Aldrich Corporation) and were machined into flags approximately 4 cm^2. Pseudoreference electrodes (Ag|AgCl) were also prepared in-house. Before each experiment, high-purity silver wire (Palmer Metals, UK (99.99%)), d = 0.5 mm, l = 5 cm) was abraded with emery paper and rinsed with deionized (Millipore) water. The silver wire was then cycled voltammetrically in 0.5 M NaCl (aqueous) before being coated with silver chloride at +0.8 V versus an SCE reference half cell (60 s). After drying, the spirally wound product was then immersed directly into the working solution. Although this generated a stable reference potential, its absolute value on the vacuum scale was not determined. High-purity nitrogen was delivered via a drying trap. Residual water was always below the level of detection of cyclic voltammetry. As a cross-check, voltammograms were routinely compared with those obtained after addition of hygroscopic fumed silica (to scavenge traces of water). No differences were observed.

Conductivity. Static conductivity measurements (constant concentration experiments) were carried out in Pyrex cells by means of

DOI: 10.1021/acssuschemeng.7b04117
ACS Sustainable Chem. Eng. 2018, 6, 2612−2620

platinized platinum conductivity probes (027−013, Jenway, UK). A digital thermometer (P755-Log, Dostmann Electronic, Wertheim, Germany) and a laboratory-built flexible glass brush stirrer were also inserted into each test cell. The temperature was maintained within ± 0.03 °C, and impedance (Z), phase angle (φ), resistance (R), and capacitance (C) values were recorded at 10 kHz using a Precision Component Analyzer (6430 A, Wayne-Kerr, UK). Absolute calibration of conductivity was against 0.01 M KCl (aqueous), 1.413 mS cm^{-1} at 25 °C. Dynamic conductivity measurements (variable concentration experiments) were carried out in a custom-designed three-necked double-walled pyrex cell (John Spray, Loughborough, UK). A platinum black conductivity probe (Mettler Toledo, UK) was inserted, along with a laboratory-built glass propeller and a Teflon tube carrying the specified diluent from a programmable syringe pump (Model 11, Harvard Apparatus Incorporated, Holliston, MA). The temperature of the system was maintained by a circulating oil bath (Julabo F26-HP, Germany); a digital thermometer (P755-Log, Dostmann Electronic, Germany) was used to monitor the temperature to an accuracy of ± 0.03 °C. Impedance (Z), phase angle (φ), resistance (R), and capacitance (C) values were typically recorded every 2 s at 10 kHz using a Precision Component Analyzer (6430 A, Wayne-Kerr Electronics, UK).

Instrumentation. Voltammograms were recorded using a μAutolab II (Metrohm, Utrecht, Netherlands).

Supercapacitors. Supercapacitors were manufactured in-house using the screen-printing method of Fletcher et al.[2−4] The electrodes consisted of 3 layers, the first layer being silver to act as the current collector. This was printed using Ercon E1660 Silver Ink (Ercon Incorporated, Wareham, MA). The second layer was a passivating carbon ink (graphite in a thermoset resin) to prevent the exposure of the silver to the working solution. The third and final layer was 1 cm^2 of activated carbon having a mean particle diameter of 10 μm (Norit DLC Supra 30, CAS [7440−44−0], Norit Americas Incorporated, Marshall, TX). The binder for the activated carbon was Kynar PVDF powder (poly(1,1-difluoroethylene), CAS [24937−79−9], Arkema France, Colombes, France). The inert substrate was typically Kapton HN polyimide film (CAS [25036−53−7], 500-gauge (127 μm), manufactured by E I Du Pont De Nemours and Co., Wilmington, DE). Glass fiber was used as the separator.

Software. Wave function Spartan '16 (2016) was used for modeling chemical structures in 3D, and Chemaxon MarvinSketch, version 5.3 (2010), was used for 2D rendering. Analysis of laboratory data was carried out using Microsoft Excel (2010). Graphs were plotted using OriginLab OriginPro, version 9.2 (2013).

RESULTS AND DISCUSSION

Initial experiments with the 60/40 mol % eutectic mixture of sulfolane and (*R*,*S*)-3-methylsulfolane (S/3MS) were concerned with establishing its effect on the conductivity of ionic liquids. Happily, BTM-TFSI was miscible in all proportions with S/3MS, so it was readily possible to analyze the full range of compositions.

Rather than carrying out a multitude of separate measurements on different mixtures of BTM-TFSI and S/3MS, we decided to automate the process using a programmable syringe pump (5 mL h^{-1}) and a frequency response analyzer. The complete apparatus was calibrated using a 0.01 M KCl (aqueous) standard solution (κ = 1.413 mS cm^{-1}) at 25 °C as shown in Figure 5.

The measured cell resistance was found to increase linearly with the volume of added water, confirming the electrical and thermal stability of the apparatus. As expected, the conductivity of KCl (aqueous) solutions decreased monotonically with increasing dilution.

The results of adding the ionic liquid BTM-TFSI to 10 mL of the 60/40 mol % eutectic mixture of sulfolane and (*R*,*S*)-3-methylsulfolane (S/3MS) are shown in Figure 6. In this case

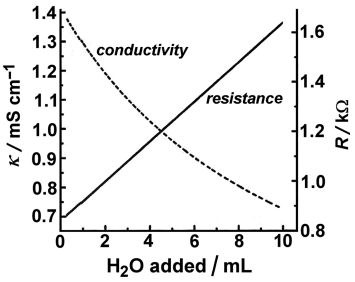

Figure 5. Calibration of conductivity apparatus using 10 mL of KCl (aqueous) (0.01 mol dm^{-3}) with addition of 10 mL of H_2O at 5 mL h^{-1}. The electrolyte conductivity (dotted line) is shown on the left-hand scale, and the cell resistance (solid line) is shown on the right-hand scale. Measurements were recorded at 2 s intervals.

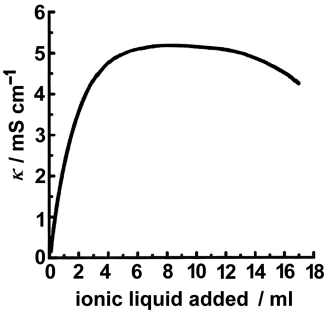

Figure 6. Conductivity versus volume of the ionic liquid BTM-TFSI added to 10 mL of a 60/40 mol % eutectic mixture of sulfolane and (*R*,*S*)-3-methylsulfolane (S/3MS) at 25 °C. Rate of continuous dilution was 5 mL h^{-1}. The 6480 points were recorded at 2 s intervals.

the conductivity peaked at 5.0 mS cm^{-1}, compared with 2.1 mS cm^{-1} for pure BTM-TFSI. Once again there was a "win−win" situation, with the diluted ionic liquid performing better than the pure ionic liquid. We attribute this counterintuitive effect to the diminishing viscosity of the solution and/or the increasing dissociation of ion pairs caused by the raised permittivity of the solution.

While an improvement in conductivity was certainly encouraging, it was nevertheless important to check that it did not occur at the expense of a diminished voltage stability window. Accordingly, we measured the one-electrode (half-cell) voltage stability window of the ternary mixture (BTM-TFSI + S/3MS) at the composition of maximum conductivity (30 mol % BTM-TFSI). The relevant data are shown in Figure 7. The gratifying result is that the one-electrode (half-cell) voltage stability window is still >3.5 V.

Figure 7 also reveals the presence of small currents (microamps) flowing immediately prior to electrolyte decomposition, at both ends of the voltammogram. Given the high sensitivity of the voltammetric technique, it is not known if these currents are due to low-level preceding electrochemical reactions or whether they are due to the presence of microtrace impurities. It is also unclear if they are related to carbon type. Further work is in progress in our laboratories to resolve this issue.

As noted earlier, the salts of asymmetric tetraalkylammonium cations such as butyltrimethyl- and hexyltriethyl- generally have freezing points <20 °C, i.e., they are liquids at room temperature, whereas the salts of symmetric tetraalkylammonium cations with TFSI, such as tetramethyl-, tetraethyl-, tetrapropyl-, and tetrabutyl-, all have melting points

DOI: 10.1021/acssuschemeng.7b04117
ACS Sustainable Chem. Eng. 2018, 6, 2612−2620

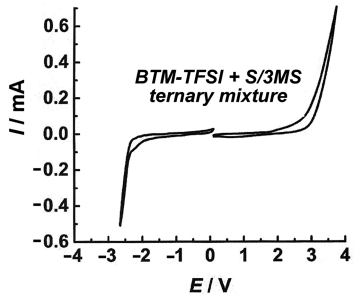

Figure 7. Current versus voltage curves depicting the one-electrode (half-cell) voltage stability window of the ternary mixture (BTM-TFSI + S/3MS) at the solution composition of maximum conductivity (30 mol % BTM-TFSI). The voltage scan rate was 100 mV s^{-1}, and the anodic and cathodic scans were recorded separately. The working electrode was a freshly polished glassy carbon disk (3.0 mm diameter). The pseudoreference electrode was Ag|AgCl|TFSI$^-$. The counter electrode was Pt gauze. The solution was N_2-saturated. Compared with that of pure BTM-TFSI, the solution conductivity has increased from 2.1 to 5.0 mS cm^{-1}.

>96 °C, i.e., they are solids at room temperature. For this reason, the salts of symmetric cations cannot be used in the pure state at room temperature.[3] However, the availability of the highly polar S/3MS eutectic now opens the possibility of using concentrated solutions of symmetric salts at 25 °C. In proof-of-concept experiments, we focused on tetraethylammonium bis(trifluorosulfonyl)imide (TEA-TFSI) because of its ready availability.

A near-saturated solution was prepared containing 43 mol % TEA TFSI in the S/3MS eutectic, and this was used as the basis for controlled dilution experiments. A typical plot of conductivity versus mole fraction is shown in Figure 8. As with the asymmetric cations, a conductivity maximum was observed, attaining the value of 5.0 mS cm^{-1} at 37 mol % TEA-TFSI.

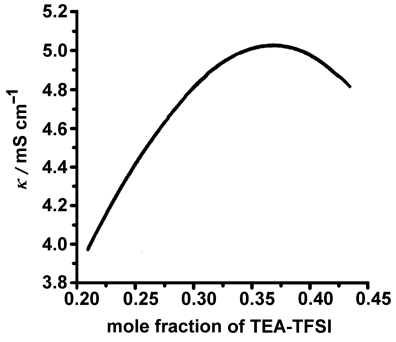

Figure 8. Conductivity versus mole fraction of TEA-TFSI in the S/3MS eutectic at 25 °C. The initial TEA-TFSI solution (43 mol %, 10 mL) was continuously diluted with S/3MS (10 mL) at 5 mL h^{-1}. The 3600 points were recorded at 2 s intervals.

For use in electric vehicles, another important factor to consider was the low temperature performance of the electrolyte in cold climates. We found that the freezing point of 37 mol % TEA-TFSI solution in the S/3MS eutectic was circa −17 °C, which is adequate for use in the UK, although it may not be adequate elsewhere. Lower temperatures would require an additional heat pack. We also measured the one-electrode (half-cell) voltage stability window of the same solution and the result is shown in Figure 9. The voltammetry of the symmetric TEA-TFSI cation is strikingly similar to that of the asymmetric BTM-TFSI cation, suggesting that it may be a cheap replacement.

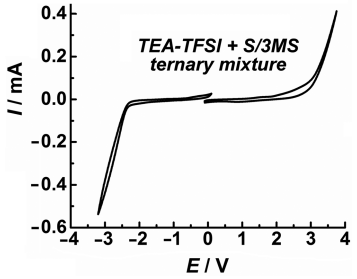

Figure 9. Current versus voltage curves demonstrating the one-electrode (half-cell) voltage stability window of the ternary mixture (TEA-TFSI + S/3MS) at the composition of maximum conductivity (37 mol % TEA-TFSI). The voltage scan rate was 100 mV s^{-1}, and the anodic and cathodic scans were recorded separately. The working electrode was a freshly polished glassy carbon disk (3.0 mm diameter). The pseudoreference electrode was Ag|AgCl|TFSI$^-$. The counter electrode was Pt gauze. The solution was N_2-saturated.

Given the favorable one-electrode (half-cell) voltammetry of the ternary mixture of TEA-TFSI with S/3MS, several two-electrode (full-cell) supercapacitors were constructed using the same composition. The electrodes were prepared by screen-printing activated carbon. Figure 10 shows the cyclic

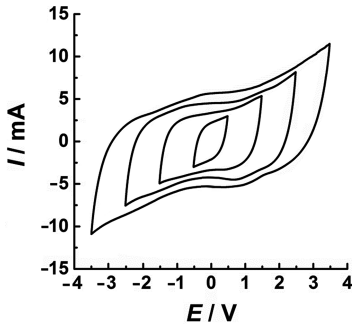

Figure 10. Current versus voltage curves for a 1 cm^2 activated carbon supercapacitor containing the ternary mixture (TEA-TFSI + S/3MS) at the composition of maximum conductivity (37 mol % TEA-TFSI). T = 25 °C. The voltage scan rate was 50 mV s^{-1}.

voltammetry at T = 25 °C. Evidently, the two-electrode (full-cell) voltage stability window is >7 V, as expected. In order to obtain steady-state data on a reasonable time scale, the scan rate was increased to 50 mV s^{-1}. This faster scan rate also magnified the nonfaradaic (capacitive) components of the current, and revealed some fine structure in the voltammetric curves. This is likely connected with the dynamic adsorption and desorption of anions and cations in different ranges of potential.

CONCLUSIONS

Binary mixtures of polar solvents and ionic liquids have long been studied as reaction media for chemical synthesis, CO_2 capture, and the stabilization of dye-sensitized solar cells.[38−44] By contrast, ternary mixtures have scarcely been discussed. In the present work we have explored the possibility of using ternary mixtures of polar solvents and ionic liquids to improve the performance of supercapacitors. Our experiments have

DOI: 10.1021/acssuschemeng.7b04117
ACS Sustainable Chem. Eng. 2018, 6, 2612−2620

revealed that it is possible to increase the conductivity of electrolytes while lowering their total economic cost. At the same time, we have confirmed earlier claims[5] that it is possible to extend the range of working temperatures far beyond the traditional liquidus range of water (0−100 °C).

In proof-of-concept experiments we have focused on ternary mixtures of sulfolane, 3-methyl sulfolane, and a series of quaternary ammonium compounds. Sulfolane was selected because of its remarkable thermal and electrochemical stability. By developing a high-precision conductivity apparatus we were able to show that the addition of a 60/40 mixture of sulfolane and 3-methyl sulfolane to the pure ionic liquid BTM-TFSI increased the solution conductivity from 2.1 to 5.0 mS cm^{-1}. Changing the anion from TFSI (bis(trifluoromethylsulfonyl)-imide) to MTC (methanetricarbonitrile) further increased the conductivity to 12.2 mS cm^{-1}. These are significant improvements.

A third method of increasing conductivity (besides adding polar solvent and switching to more mobile ions) was to raise the temperature of the system. This was made possible by the availability of our thermally stable electrolytes. The remarkable result is shown in Figure 11, where it can be seen that an increase in measured capacitance accompanies the increase in temperature. The same trend is observed in the absence of sulfolane (Figure 12) indicating that the solvent is not the main factor responsible. Such an increase in measured capacitance contrasts sharply with the behavior of dielectric solids, for which the measured capacitance decreases with increasing temperature.

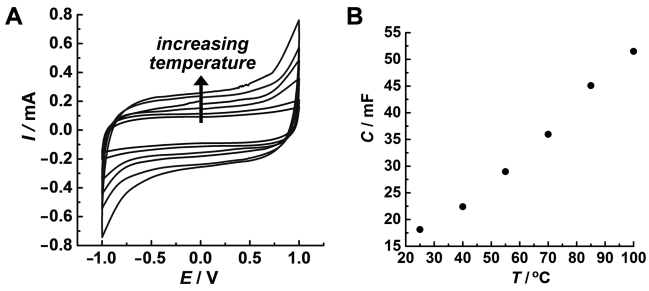

Figure 11. (A) Current versus voltage curves for a 1 cm^2 activated carbon supercapacitor containing the ternary mixture (TEA-TFSI + S/3MS) having maximum conductivity (37 mol % TEA-TFSI). The voltage scan rate was 5 mV s^{-1}. T = 25, 40, 55, 70, 85, and 100 °C. (B) Variation of measured capacitance with temperature.

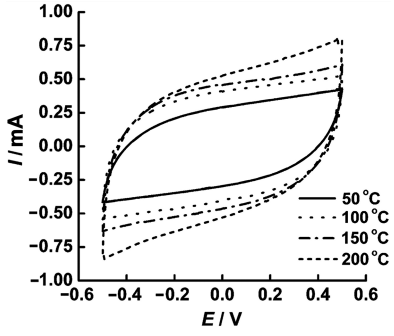

Figure 12. Current versus voltage curves for a 1 cm^2 activated carbon supercapacitor containing solvent-free butyltrimethylammonium bis-(trifluoromethylsulfonyl)imide (BTM-TFSI). The voltage scan rate was 5 mV s^{-1}. T = 50, 100, 150, and 200 °C. In this case, a narrow (1.0 V) window was selected to allow voltammetry to be recorded at 200 °C without electrolyte decomposition.

In the present work, we attribute the positive temperature coefficient of measured capacitance to the presence of a wide distribution of RC time constants in the activated carbon electrodes, something we have also identified as the cause of nonexponential charge/discharge kinetics.[4,28] The equivalent circuit is a vertical ladder network, which associates each small element of electroactive area with a unique conduction pathway through the porous mass of the electrode (Figure 13). Thus, each patch of electroactive surface has its own RC time constant.

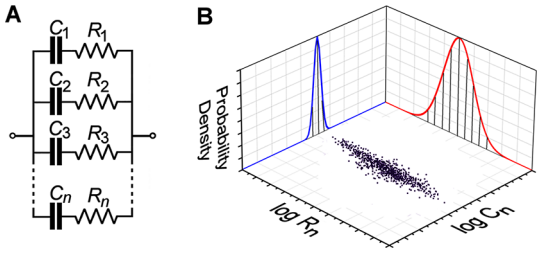

Figure 13. (A) Proposed equivalent circuit of an activated carbon electrode. (B) Idealized representation of the joint distribution of log R_n and log C_n values. Each point on the plane corresponds to one rung on the ladder network. Note that there is a much wider spread of log R_n than log C_n values.

Order-of-magnitude estimates of R and C may be derived from the textbook formulas for the resistance and capacitance of a single cylindrical pore, neglecting access resistance:

$$R = \frac{L}{\pi r^2 \kappa_p} \tag{1}$$

and

$$C = 2\pi r L C_s \tag{2}$$

Here, R is the resistance of the pore (Ω), L is the length of the pore (m), r is the radius of the pore (m), and κ_p is the conductivity of the pore (S m^{-1}). In addition, C is the capacitance of the pore (F), and C_s is the areal capacitance of the pore wall (F m^{-2}). Inserting realistic values (L = 10 μm, r = 1 nm, κ_p = 1 S m^{-1}, and C_s = 4 μF cm^{-2}), one readily finds that $R \approx 10^{12}$ Ω (teraohms) and $C \approx 10^{-15}$ F (femtofarads). This implies that $RC \approx 10^{-3}$ s (milliseconds). Such a rapid charging of an activated carbon supercapacitor has never been observed experimentally, something which must be due to either (i) a C_s value about 10^3 times larger than 4 μF cm^{-2} or (ii) a κ_p value about 10^3 times smaller than 1 S m^{-1}. In our view, the second explanation is more likely, given the existence of Donnan Exclusion in charged pores of nanometer dimensions.[45,46]

As is well-known, every charged interface attracts a population of counter-ions to form an electrical double layer. In liquid-filled pores of nanometer dimensions, the electrical double layer typically spans the entire width of the nanopores, resulting in dramatic changes in their internal composition. Indeed, to maintain electroneutrality, the charges inside the nanopore walls Coulombically expel any mobile charges of the same sign (the coions) into the nearby solution and Coulombically attract mobile charges of the opposite sign (the counter-ions). As a result, there is a major loss of intrapore conductivity κ_p. We believe this classical effect is

DOI: 10.1021/acssuschemeng.7b04117
ACS Sustainable Chem. Eng. 2018, 6, 2612−2620

sufficient to account for the 1000-fold discrepancy between the predicted and observed response times of activated carbon nanopores and thus provides the explanation for the slower-than-expected charging observed at room temperature. By contrast, raising the temperature far above room temperature lowers the *RC* time constants of the pores and allows more of them to respond on the time scale of experiments.

Figures 11 and 12 also furnish important new insights into the utilization of active material. Evidently, at least 50% of the surface area of activated carbon electrodes is functionally useless at room temperature on account of the nanopores being too narrow or too deep. This is crucial information for the improvement of supercapacitor devices, and also for supercapacitor modeling.[47−51]

Multiplying eqs 1 and 2 together, and defining a response time $\tau = RC$, one obtains

$$\tau = \frac{C_s}{\kappa_p}\frac{2L^2}{r} \tag{3}$$

This equation reveals that the response time of a single nanopore can be shortened in two ways: (i) by increasing the nanopore radius r or (ii) by decreasing the nanopore length L. However, the fact that the response time depends on the square of the nanopore length suggests that the latter may be the easier target for improvement.

At this point, the low utilization of surface area in activated carbon electrodes may be compared with theoretical estimates. For a carbon−carbon interatomic distance of 0.1421 nm,[52] each graphene hexagon has an area of 0.05246 nm^2, implying that a full plane of graphene has a specific surface area of 1315 m^2g^{-1}, or 2630 m^2g^{-1} if both sides are exposed simultaneously. However, since only one side is thought to be accessible on the surface of activated carbon due to sp^3 cross-linking between the layer planes,[2] we may reasonably conclude that the "one-sided" value of 1315 m^2g^{-1} is the maximum attainable specific surface area. Larger values reported in the literature are most likely due to the naïve application of Brunauer−Emmett−Teller theory to microporous solids. As noted by the International Organization for Standardization in 2010, "the specific surface area obtained by applying the BET method to adsorption isotherms from microporous solids does not reflect the true internal surface area."[53] Given the reported estimates[54−56] of basal plane areal capacitance of 2−4 μF cm^{-2}, 4−8 μF cm^{-2}, and 10 μF cm^{-2}, we are led inexorably to the conclusion that the maximum specific capacitance of activated carbon is in the range of 50−150 F g^{-1}. This means that claimed values greater than 150 F g^{-1} should be regarded with a high degree of skepticism.[57−62] Finally, we also note that cylindrical pores having diameters less than ∼0.7 nm cannot physically accommodate enough counterions to fully charge the pore walls, so counter ion starvation may also be occurring in addition to Donnan Exclusion.

AUTHOR INFORMATION

Corresponding Author

*E-mail: I.Kirkpatrick@lboro.ac.uk. Tel.: +44-(0)1509-227-265. Fax: +44-(0)1509-227-275.

ORCID

Iain Kirkpatrick: 0000-0002-9722-8399

Notes

The authors declare no competing financial interest.

ACKNOWLEDGMENTS

This work was sponsored by the EPSRC (UK) Grant Number EP/M009394/1, "Electrochemical Vehicle Advanced Technology" (ELEVATE). We also thank John Spray and Mark Edgar for valuable conversations.

REFERENCES

(1) *EPSRC's £6 million to drive new Low Carbon Vehicle Technologies Research*. https://www.epsrc.ac.uk/newsevents/news/lowcarbonvehicletech. September 10, 2014.

(2) Fletcher, S. Screen-Printed Carbon Electrodes. In *Electrochemistry of Carbon Electrodes*; Alkire, R. C., Bartlett, P. N., Lipkowski, J., Eds.; Wiley-VCH: Hoboken, NJ, 2015; pp 419−439.

(3) Fletcher, S.; Black, V. J.; Kirkpatrick, I.; Varley, T. S. Quantum design of ionic liquids for extreme chemical inertness and a new theory of the glass transition. *J. Solid State Electrochem.* **2013**, *17* (2), 327−337.

(4) Fletcher, S.; Black, V. J.; Kirkpatrick, I. A universal equivalent circuit for carbon-based supercapacitors. *J. Solid State Electrochem.* **2014**, *18* (5), 1377−1387.

(5) Fletcher, S.; Black, V. J. [Schlumberger Technology Corporation] High Temperature Supercapacitor. U.S. Patent 9,318,271 B2, June 21, 2012.

(6) Barton, A. F. M. *Handbook of Solubility Parameters and other Cohesion Parameters*, 2nd ed.; CRC Press: Boca Raton, FL, 1983.

(7) Lide, D. R. *Handbook of Organic Solvents*; CRC Press: Boca Raton, FL, 1994.

(8) Abboud, J.-L.M.; Notari, R. Critical compilation of scales of solvent parameters. Part I. Pure, non-hydrogen bond donor solvents (Technical Report). *Pure Appl. Chem.* **1999**, *71* (4), 645−718.

(9) Yaws, C. L. *Thermophysical Properties of Chemicals and Hydrocarbons*, 2nd ed.; Elsevier/Gulf Professional Publishing: Oxford, U.K., 2014.

(10) Vaughn, J. W.; Hawkins, C. F. Physical Properties of Tetrahydrothiophene-1, 1-Dioxide and 3-Methyltetrahydrothiophene-1, 1-Dioxide. *J. Chem. Eng. Data* **1964**, *9* (1), 140−142.

(11) Delfs, D. [IG Farbenindustrie AG] *Verfahren zur Herstellung von Ab kommlingen der Cyclotetramethylensulfons*. [Process for the preparation of derivatives of cyclotetramethylenesulfone] German Patent 682,079, January 23, 1937.

(12) Farlow, M. W. [E. I. duPont de Nemours and Co.] Process for the production of 2,3,4,5-tetrahydrothiophene-1,1-dioxide. U.S. Patent 2,233,999 A, April 30, 1940.

(13) Morris, R. C.; Melchior, N. C. [Shell Development Company] Hydrogenation of unsaturated cyclic sulfones. U.S. Patent 2,451,298 A, November 27, 1943.

(14) Evans, T. W.; Morris, R. C. [Shell Development Company] Solvent Extraction Process, U.S. Patent 2,360,859, February 8, 1943.

(15) Durrum, E. L. [Shell Development Company] Process for separating aromatic hydrocarbons. U.S. Patent 2,407,820 A (23 Mar 1943).

(16) Stewart, O. *Sulfolane Technical Assistance and Evaluation Report*; Alaska Department of Environmental Conservation: Anchorage, AK, 2010.

(17) Van Tassell, H. M. [Universal Oil Products Company Recovery of sulfolane by distillation with pre-vaporization. U.S. Patent 3,396,090, June 29. 1966.]

(18) Deal, C. H., Jr.; Dunn, C. L.; Hill, E. S.; Papadopoulos, M. N.; Zarker, K. E. Sulfinol - A New Process for Gas Purification. In *6th World Petroleum Congress: Proceedings*, Frankfurt am Main, Germany, 19−26 June, 1963; World Petroleum Council: London, 1963; Section IV, Paper 32. [Sulfinol is a registered trademark of Shell Global Solutions.]

(19) *Canadian Soil Quality Guidelines for the Protection of Environmental and Human Health*; Canadian Council of Ministers of the Environment: Ottawa, Ontario, Canada, 2006.

DOI: 10.1021/acssuschemeng.7b04117
ACS Sustainable Chem. Eng. 2018, 6, 2612−2620

(20) Martinma, J. Sulfolane. In *The Chemistry of Nonaqueous Solvents*; Lagowski, J. J., Ed.; Solution Phenomena and Aprotic Solvents; Academic Press Inc, New York, 1976; Vol. *IV*, pp. 248−288.
(21) Chappelow, C. C.; Christie, H. W.; Byerley, T. J.; Cooper, G. R. *Physicochemical Evaluations of Selected Solvents for Use in Decontaminating Agent "Multipurpose (DAM) Formulation"*; Report Number ERDC-CR-107; The Edgewood Research Development and Engineering Center (ERDEC), US Army Chemical and Biological Defense Command: Kansas City MO, 1994.
(22) von Hofmann, A. W. Beiträge zur Kenntniss der flüchtigen organischen Basen. *Annalen der Chemie und Pharmacie* **1851**, *78* (3), 253−286.
(23) Stevens, T.; Creighton, E. M.; Gordon, A. B.; MacNicol, M. CCCCXXIII.—Degradation of quaternary ammonium salts. Part I. *J. Chem. Soc.* **1928**, *0*, 3193−3197.
(24) De La Zerda, J.; Neumann, R.; Sasson, Y. Hofmann decomposition of quaternary ammonium salts under phase-transfer catalytic conditions. *J. Chem. Soc., Perkin Trans. 2* **1986**, No. 6, 823−826.
(25) Maton, C.; De Vos, N.; Stevens, C. V. Ionic liquid thermal stabilities: decomposition mechanisms and analysis tools. *Chem. Soc. Rev.* **2013**, *42* (13), 5963−5977.
(26) Arvai, R.; Toulgoat, F.; Langlois, B. R.; Sanchez, J. Y.; Médebielle, M. A simple access to metallic or onium bistrifluoromethanesulfonimide salts. *Tetrahedron* **2009**, *65* (27), 5361−5368.
(27) Trofimenko, S.; Little, E. L., Jr; Mower, H. F. Tricyanomethane (cyanoform), carbamyldicyanomethane, and their derivatives. *J. Org. Chem.* **1962**, *27* (2), 433−438.
(28) Fletcher, S.; Kirkpatrick, I.; Dring, R.; Puttock, R.; Thring, R.; Howroyd, S. The modelling of carbon-based supercapacitors: distributions of time constants and Pascal equivalent circuits. *J. Power Sources* **2017**, *345*, 247−253.
(29) Yoshida, Y.; Muroi, K.; Otsuka, A.; Saito, G.; Takahashi, M.; Yoko, T. 1-Ethyl-3-methylimidazolium based ionic liquids containing cyano groups: synthesis, characterization, and crystal structure. *Inorg. Chem.* **2004**, *43* (4), 1458−1462.
(30) Wooster, T. J.; Johanson, K. M.; Fraser, K. J.; MacFarlane, D. R.; Scott, J. L. Thermal degradation of cyano containing ionic liquids. *Green Chem.* **2006**, *8* (8), 691−696.
(31) Martins, V. L.; Rennie, A. J.; Torresi, R. M.; Hall, P. J. Ionic liquids containing tricyanomethanide anions: physicochemical characterisation and performance as electrochemical double-layer capacitor electrolytes. *Phys. Chem. Chem. Phys.* **2017**, *19* (25), 16867−16874.
(32) Jarosik, A.; Krajewski, S. R.; Lewandowski, A.; Radzimski, P. Conductivity of ionic liquids in mixtures. *J. Mol. Liq.* **2006**, *123* (1), 43−50.
(33) Ruiz, V.; Huynh, T.; Sivakkumar, S. R.; Pandolfo, A. G. Ionic liquid-solvent mixtures as supercapacitor electrolytes for extreme temperature operation. *RSC Adv.* **2012**, *2* (13), 5591−5598.
(34) Kalugin, O. N.; Voroshylova, I. V.; Riabchunova, A. V.; Lukinova, E. V.; Chaban, V. V. Conductometric study of binary systems based on ionic liquids and acetonitrile in a wide concentration range. *Electrochim. Acta* **2013**, *105*, 188−199.
(35) Silva, F. T.; Lima, D. W.; Becker, M. R.; Souza, R. F.; Martini, E. Transport properties of binary solutions containing the ionic liquid BMI-BF4 and ethylene glycol. *J. Braz. Chem. Soc.* **2015**, *26* (10), 2125−2129.
(36) Ueno, K.; Murai, J.; Ikeda, K.; Tsuzuki, S.; Tsuchiya, M.; Tatara, R.; Mandai, T.; Umebayashi, Y.; Dokko, K.; Watanabe, M. Li(+) solvation and ionic transport in lithium solvate ionic liquids diluted by molecular solvents. *J. Phys. Chem. C* **2016**, *120* (29), 15792−15802.
(37) Papancea, A.; Paţachia, S.; Porzsolt, A. Conductivity studies of imidazolium-based ionic liquids in aqueous solution. *Bull. Transilvania Univ. Brasov, Ser. I*, **2015**, *8*, 67−72.
(38) Hallett, J. P.; Welton, T. Room-temperature ionic liquids: solvents for synthesis and catalysis. 2. *Chem. Rev.* **2011**, *111* (5), 3508−3576.
(39) Yang, J.; Yu, X.; Yan, J.; Tu, S. T. CO_2 capture using amine solution mixed with ionic liquid. *Ind. Eng. Chem. Res.* **2014**, *53* (7), 2790−2799.
(40) Gorlov, M.; Kloo, L. Ionic liquid electrolytes for dye-sensitized solar cells. *Dalton Trans.* **2008**, *20*, 2655−2666.
(41) Mancini, P. M.; Fortunato, G. G.; Vottero, L. R. Molecular solvent/ionic liquid binary mixtures: designing solvents based on the determination of their microscopic properties. *Phys. Chem. Liq.* **2004**, *42* (6), 625−632.
(42) Marsh, K. N.; Boxall, J. A.; Lichtenthaler, R. Room temperature ionic liquids and their mixtures—a review. *Fluid Phase Equilib.* **2004**, *219* (1), 93−98.
(43) Stoppa, A.; Hunger, J.; Buchner, R. Conductivities of binary mixtures of ionic liquids with polar solvents. *J. Chem. Eng. Data* **2009**, *54* (2), 472−479.
(44) Niedermeyer, H.; Hallett, J. P.; Villar-García, I. J.; Hunt, P. A.; Welton, T. Mixtures of ionic liquids. *Chem. Soc. Rev.* **2012**, *41* (23), 7780−7802.
(45) Nic, M.; Jirat, J.; Kosata, B. Donnan Exclusion. In *Compendium of Chemical Terminology (Gold Book)*, version 2.3.3; International Union of Pure and Applied Chemistry: Research Triangle Park, NC, 2014.
(46) Balme, S.; Picaud, F.; Manghi, M.; Palmeri, J.; Bechelany, M.; Cabello-Aguilar, S.; Abou-Chaaya, A.; Miele, P.; Balanzat, E.; Janot, J. M. Ionic transport through sub-10 nm diameter hydrophobic high-aspect ratio nanopores: experiment, theory and simulation. *Sci. Rep.* **2015**, *5*, 1−14.
(47) Kroupa, M.; Offer, G. J.; Kosek, J. Modelling of Supercapacitors: Factors Influencing Performance. *J. Electrochem. Soc.* **2016**, *163* (10), A2475−A2487.
(48) Pilon, L.; Wang, H.; d'Entremont, A. Recent advances in continuum modeling of interfacial and transport phenomena in electric double layer capacitors. *J. Electrochem. Soc.* **2015**, *162* (5), A5158−A5178.
(49) Bandlamudi, S. R. P.; Cooney, M. J.; Martin, G. L.; Benjamin, K. M. Molecular Simulation and Experimental Characterization of Ionic-Liquid-Based Cosolvent Extraction Solvents. *Ind. Eng. Chem. Res.* **2017**, *56* (11), 3040−3048.
(50) Liu, K.; Wu, J. Boosting the Performance of Ionic-Liquid-Based Supercapacitors with Polar Additives. *J. Phys. Chem. C* **2016**, *120* (42), 24041−24047.
(51) Yang, H.; Yang, J.; Bo, Z.; Chen, X.; Shuai, X.; Kong, J.; Yan, J.; Cen, K. Kinetic-Dominated Charging Mechanism within Representative Aqueous Electrolyte-based Electric Double-Layer Capacitors. *J. Phys. Chem. Lett.* **2017**, *8* (15), 3703−3710.
(52) McCreery, R. L. In *Electroanalytical Chemistry: A Series of Advances*; Bard, A. J., Ed.; Dekker: New York, 1991; Vol. *17*, pp 221−374.
(53) Annex C (informative). Surface area of microporous materials. In *Determination of the specific surface area of solids by gas adsorption — BET method*; International Standard ISO 9277: 2010, 2nd ed; ISO Central Secretariat: Geneva, Switzerland, 2010. https://www.iso.org/standard/44941.html.
(54) Randin, J.-P.; Yeager, E. Differential capacitance study on the basal plane of stress-annealed pyrolytic graphite. *J. Electroanal. Chem. Interfacial Electrochem.* **1972**, *36*, 257−276.
(55) Zou, Y.; Walton, A. S.; Kinloch, I. A.; Dryfe, R. A. Investigation of the Differential Capacitance of Highly Ordered Pyrolytic Graphite as a Model Material of Graphene. *Langmuir* **2016**, *32* (44), 11448−11455.
(56) Lobato, B.; Suárez, L.; Guardia, L.; Centeno, T. A. Capacitance and surface of carbons in supercapacitors. *Carbon* **2017**, *122*, 434−445.
(57) Chmiola, J.; Yushin, G.; Dash, R.; Gogotsi, Y. Effect of pore size and surface area of carbide derived carbons on specific capacitance. *J. Power Sources* **2006**, *158* (1), 765−772.
(58) Simon, P.; Burke, A. F. Nanostructured carbons: double-layer capacitance and more. *Interface* **2008**, *17* (1), 38−43.

DOI: 10.1021/acssuschemeng.7b04117
ACS Sustainable Chem. Eng. 2018, 6, 2612−2620

(59) Simon, P.; Gogotsi, Y. Charge storage mechanism in nanoporous carbons and its consequence for electrical double layer capacitors. *Philos. Trans. R. Soc., A* **2010**, *368*, 3457−3467.
(60) Zhang, Y.; Zhang, Y.; Huang, J.; Du, D.; Xing, W.; Yan, Z. Enhanced Capacitive Performance of N-Doped Activated Carbon from Petroleum Coke by Combining Ammoxidation with KOH Activation. *Nanoscale Res. Lett.* **2016**, *11* (1), 1−7.
(61) Piñeiro-Prado, I.; Salinas-Torres, D.; Ruiz-Rosas, R.; Morallón, E.; Cazorla-Amorós, D. Design of activated carbon/activated carbon asymmetric capacitors. *Front. Mater.* **2016**, *3*, 1−12.
(62) Li, Y.; Ren, R. Q.; Jin, X. J. Effect of Sulfur Impregnation Temperature on Properties of N-Doped Activated Carbon for Supercapacitor Applications. *Int. J. Electrochem. Sci.* **2016**, *11* (11), 9599−9613.

DOI: 10.1021/acssuschemeng.7b04117
ACS Sustainable Chem. Eng. 2018, 6, 2612−2620